Article

Statistical Analysis and Optimization of the Experimental Results on Performance of Green Aluminum-7075 Hybrid Composites

Olanrewaju Seun Adesina [1,*], Abayomi Adewale Akinwande [2,*] , Oluwatosin Abiodun Balogun [2] ,
Adeolu Adesoji Adediran [3,4] , Olufemi Oluseun Sanyaolu [1] and Valentin Romanovski [5,6]

[1] Department of Mechanical Engineering, Redeemer's University, Ede 232101, Osun State, Nigeria
[2] Department of Metallurgical and Materials Engineering, Federal University of Technology,
   Akure 340110, Ondo State, Nigeria
[3] Department of Mechanical Engineering, Landmark University, Omu-Aran 251103, Kwara State, Nigeria
[4] Department of Mechanical Engineering Science, University of Johannesburg, Johannesburg 2092, South Africa
[5] Center for Functional Nano-Ceramics, National University of Science and Technology, "MISIS", Lenin Av., 4,
   119049 Moscow, Russia
[6] Department of Materials Science and Engineering, University of Virginia, Charlottesville, VA 22904, USA
* Correspondence: osaadesina@gmail.com (O.S.A.); abypublications@gmail.com (A.A.A.)

Abstract: The present study assessed the potential of engaging response surface analysis in the experimental design, modeling, and optimization of the strength performance of aluminum-7075 green composite. The design of the experiment was carried out via the Box–Behnken method and the independent variables are rice husk ash (RHA) at 3–12 wt.%, glass powder (GP) at 2–10 wt.%, and stirring temperature (ST) at 600–800 °C. Responses examined are yield, ultimate tensile, flexural, and impact strengths, as well as microhardness and compressive strength. ANOVA analysis revealed that the input factors had consequential contributions to each response, eventually presenting regression models statistically fit to represent the experimental data, further affirmed by the diagnostic plots. The result of the optimization envisaged an optimal combination at 7.2% RHA, 6.2 GP, and 695 °C with a desirability of 0.910. A comparison between the predicted values for the responses and the values of the validation experiment revealed an error of <5% for each response. Consequently, the models are certified adequate for response predictions at 95% confidence, and the optimum combination is adequate for the design of the composite.

1. Introduction

Modern-day engineering applications have centered on the use of aluminum alloys owing to their light weight, strength, and excellent corrosion properties. Aluminum metal matrix composites (AMMCs) are often preferred to unreinforced base aluminum metal because of their superior strength, hardness, and wear resistance. These have made AMMCs more attractive for engineering applications than unreinforced ones. In recent times, hybrid AMMCs containing two or more reinforcing fillers have been preferred over single AMMCs because of their superior mechanical performance [1,2]. These sets of composites are engaged in defense, aerospace, automobiles, trains, and other forms of application. Various studies have been engaged in the fabrication of hybrid AMMCs using synthetic reinforcement [3–10].

Owing to high cost of these reinforcing particles and for the purpose of developing sustainable hybrid aluminum composite, bio- and industrial wastes are often reprocessed in powdered form and applied as supplements alongside synthetic fillers in aluminum matrixes. For instance, in Vijayakumar et al. [11], aluminum-5083 was hybridized with SiC and fly ash via stir casting. While fly ash was held constant at 2 wt.%, SiC was varied at 3, 5, and 7 wt.%. Tensile strength and hardness were reported to improve as SiC dosage

increased to 3 and 5%, while 7 wt.% SiC engendered a slight reduction in the strength and hardness. Impact strength improved with the SiC addition between 3 and 5 wt.% and remained constant at 7 wt.%. Dwivedi et al. [12] combined SiC and RHA as supplements in the Al-6061 matrix. Both were combined in proportions of 2.5, 5, 7.5, 10, 12.5, and 15 wt.%, respectively. The tensile performance was reported to peak when combining 12.5% SiC and 2.5% RHA. Meanwhile, peak hardness was reported when 15% SiC was introduced, of which, ductility reduced progressively with the addition of the reinforcement. Equally, Singh et al. [13] experimented with using eggshell bioash as a supplement filler for B_4C in ZA-27. The two were combined at 1.25, 2.5, 3.75, and 5 wt.%, respectively. As B_4C increased and eggshell ash decreased, porosity was reported to increase. Brinell hardness, tensile strength, and compressive strength peaked when combining 1.25 wt.% eggshell ash with 3.75 wt.% B_4C, while elongation reduced with the addition of the fillers when compared with the base alloy. In the investigation carried out by Mugutkar et al. [14], rice husk ash (RHA) was varied at 5, 10, and 15 wt.% as a supplement particulate to B_4C, which was maintained at 2 wt.%. The result showed that peak tensile and compressive strengths were recorded at 15 wt.% RHA. Meanwhile, hardness was shown to depreciate with an increase in RHA. Other studies entailing agro-industrial fillers in aluminum alloy matrixes are Subramaniam et al. [15]; Dwivedi and Dwivedi [16].

Glass waste is an industrial and environmental waste that is non-biodegradable, and its presence in landfills has resulted in environmental degradation. Some investigations on the recycling of this waste into aluminum matrixes in powder form have been carried out. Studies on waste glass particles as reinforcing particles in aluminum matrix are in [17–19]. Each of the investigations revealed how the properties of the base aluminum alloy were improved as the glass powder was introduced. However, there are few studies that considered it in combination with another reinforcement. Additionally, in [17–19], parameters of particulates are varied; however, variation in casting temperatures was not recorded. Casting temperatures play an important role in the properties of a finished cast product because of their effect on the viscosity and particle distribution of the particles within the melt, which eventually affect the mechanical performance of the final product. The present investigation was conceived to study the influence of RHA proportion, waste glass dosage, and casting temperature on mechanical performance of Al-7075 prepared by the stir casting technique.

In the reviewed studies, there was no optimal combination of the reinforcing variables for optimal resultant performance of the hybrid composite. Recent studies involving two or more variables were carried out to achieve optimum mix proportion for optimal performance. Furthermore, current studies are engaging in the statistical analysis of experimental results and mathematical modeling of the outcome for future results predictions [20,21]. This approach has been taken in studies such as refs [22–25]. In a parallel study, we strengthened pure AA-7075 with rice husk ash and glass powder in the fabrication of green AA-7075 composite. In the study, we analyzed the effect of three variables: rice husk ash (A), glass powder (B), and stirring temperature (C) on the microstructure and mechanical performance of the composite. Since three experimental variables were involved, the full experimental design would involve $3^3 = 27$ experimental runs. Towards reducing the cost in carrying out 27 experimental runs, the Box–Behnken method of the response surface technique was engaged in the design of experiment which involved 14 experimental runs. The account of the parallel study was based on experimental observation. However, the account lacks statistical analysis, modeling, and optimization of the result, which could not be presented because of the volume limitation of the report. The present study therefore showcases ANOVA analysis, regression models, optimization, and validation procedures carried out on the experimental outcomes. The statistical analysis showed how much influence the experimental variables (A, B, and C) had on the experimental outcomes, and with the mathematical models, future predictions can be made, which in turn can reduce experimental cost. Furthermore, the experimental report could not present the optimal

combination of the three parameters that can yield optimal mechanical performance of the composite, which is addressed in the present report.

2. Experimental Program

The experimental program entails the design of experiment, and statistical analysis of experimental results on AA-7075/RHA/GP composite.

2.1. Design of Experiment (DoE)

Box–Behnken design, often known as BBD, is an approach to the response surface technique that was employed in the experiment's design. The independent factors include the quantity of rice husk ash (A), the amount of glass powder (B), and the temperature at which the mixture is being stirred (C). Through the use of mathematical and statistical approaches [26–28], the response surface approach investigates the interactions that may take place between a number of different variables and a number of different responses. In order to analyze the interactions, several approaches are used. The contributions of Design-Expert 13 were essential for both the initial stage of preparing the experiment and the subsequent phase of analyzing the outcomes. In all, there were fourteen (14) distinct experimental runs that were conducted and assessed with reference to the many varied response parameters. In Table 1, the three levels of the experimental components that were incorporated into the design of the experiment are shown, and in Table 2, fourteen different combinations of the variables that were investigated are displayed.

Table 1. Levels of the experimental factors.

Factors	Low Level	Medium Level	High Level
Rice husk ash (A wt.%)	3	7.5	12
Glass powder (B wt.%)	2	6	10
Casting temperature (°C)	600	700	800

Table 2. Variable distribution in the design of experiment.

Experimental Runs	Coded Levels			Variable Combination		
	A	**B**	**C**	**A (wt.%)**	**B (wt.%)**	**C (°C)**
1	1	0	−1	3	2	700
2	−1	1	0	7.5	2	800
3	−1	0	1	3	10	700
4	−1	0	−1	7.5	10	600
5	1	0	1	12	6	800
6	0	−1	1	7.5	6	700
7	0	0	0	7.5	2	600
8	0	0	0	12	10	700
9	0	−1	−1	3	6	800
10	0	1	−1	12	6	600
11	−1	−1	0	12	2	700
12	1	1	0	7.5	6	700
13	0	0	0	7.5	10	800
14	1	−1	0	3	6	600

A is rice husk ash proportion, B is glass powder dosage, C is casting temperature.

2.2. A Brief on Composite Development and Examined Properties

Table 1 details the chemical makeup of the 7075-T6 aluminum ingot that was acquired for the experiment. Glass powder was produced by shattering collected and discarded glass into tiny fragments, then grinding and milling the fragments into powder. Procured rice husk was initially washed, dried, and heated in a muffle furnace at 700 °C for 6 h to obtain the ash, which was then crushed and sieved to 23 microns. The procured AA-7075 billet was charged into a graphite crucible (dimensions 100 mm in diameter and 175 mm in

height), which was initially preheated to 500 °C. Prior to the casting procedure, RHA and GP were preheated to 500 °C.

The temperature was raised to the specified levels (Table 2). The melt was stirred at 300 revolutions per minute, and preheated fillers (RHA and GP) were introduced into the resulting vortex. The filler discharge rate was kept at a rate of 2.5 g/min. Each mixture was stirred for 10 min at 300 rpm. Subsequently, the molten liquid of the composites was poured at a rate of 2.4 cm^3/s into metal molds, and the solidification rate was kept constant at 100 K/s. The resulting specimens were tested with tensile, flexural, hardness, impact, and compression tests as per ASTM E 8/E8M-21 [29], ASTM A 370 [30], ASTM E 384-11 [31], ASTM E 311 [32], and ASTM E09-9 [33], respectively. Obtained experimental results were recorded against each experimental run as presented in Table 3.

Table 3. Experimental results realized at variable combinations.

Experimental Runs	Variable Combinations				Responses					
	A (wt.%)	B (wt.%)	C (°C)	Designation	YS	UTS	FS	HD	IS	CS
1	3	2	700	3/2/700	400	450	134	458	5.52	352
2	7.5	2	800	7.5/2/800	397	440	136	360	4.49	308
3	3	10	700	3/10/700	405	456	184	318	4.48	550
4	7.5	10	600	7.5/10/600	402	450	162	365	5.54	596
5	12	6	800	12/6/800	260	314	181	348	4.06	312
6	7.5	6	700	7.5/6/700	610	697	177	550	7.54	606
7	7.5	2	600	7.5/2/600	502	552	127	410	6.49	396
8	12	10	700	12/10/700	255	306	205	320	3.00	600
9	3	6	800	3/6/800	404	449	162	351	4.51	252
10	12	6	600	12/6/600	350	398	156	406	4.83	392
11	12	2	700	12/2/700	350	401	162	360	4.03	400
13	7.5	10	800	7.5/10/800	307	354	195	314	3.52	497
13	7.5	6	700	7.5/6/700	608	712	178	547	7.53	610
14	3	6	600	3/6/600	497	446	135	406	6.48	346

3. Results and Statistical Analysis

3.1. Property Responses of Composites

Rice husk ash proportion is denoted by the letter A, glass powder dosage by the letter B, casting temperature by the letter C, yield strength by the letter Y, ultimate tensile strength by UTS, flexural strength by FS, microhardness by Hv, impact strength by IS, and compressive strength by CS (MPa).

3.2. Statistical Analysis of Experimental Outcome

An analysis of variance (ANOVA), computational analysis, validation of the model, response surface analysis, and optimization were all performed on the obtained experimental data.

3.2.1. Analysis of Variance (ANOVA)

In order to have an idea of whether or not the differences that were found in the data are statistically significant, analyses of variance were carried out. The assessment was carried out at a degree of confidence of 95% and a level of significance of 5%. To serve as the foundation for establishing the relevance of a particular parameter or interaction, a probability value, denoted by *p*, was selected. If the *p*-value is less than 0.05, this implies that the contribution is significant. When the value is more than 0.05, on the other hand, the contribution is considered to be negligible.

The findings of the ANOVA on the responses are summarized in Table 4. The *p*-values for the models of the response variables are less than 0.05, indicating that the models adequately capture the data. The residual coefficient of correlation for the models is 0.9905, which is more than 0.95, indicating that there is a good connection between the models

and the corresponding data. As a result, the models have a reliability of more than 95% to describe the data with a standard deviation of less than 5%. In addition to this, the *p*-values for the mismatch are higher than 0.05. As a consequence of this, the models exhibit a high level of fitting in relation to the residuals. The discrepancy between the modified R^2 and the expected R^2 is less than 0.2 (which is less than 20 percent), which provides more evidence that the model is statistically fit. The fact that the value of the adequacy accuracy for the responses is greater than 4 indicates that the models may be used to navigate the design space.

Table 4. ANOVA on responses.

Source	TS	UTS	FS	HD	IS	CS
Model	<0.0001	<0.0001	<0.0001	<0.0001	<0.0001	<0.0001
A—RHA	<0.0001	0.0005	0.0841	<0.0001	<0.0001	<0.0001
B—GP	0.0012	0.0033	0.0009	<0.0001	0.0003	<0.0001
C—Temperature	0.0002	0.0026	0.0034	<0.0001	<0.0001	<0.0001
AB	0.0328	0.0588	0.0238	0.3348	0.982	0.8325
AC	0.9388	0.0933	0.9337	0.7759	0.0229	0.1682
BC	0.7983	0.7315	0.9779	0.0093	0.9281	0.2665
A^2	<0.0001	<0.0001	<0.0001	0.9184	<0.0001	<0.0001
B^2	<0.0001	<0.0001	<0.0001	0.0833	<0.0001	0.1722
C^2	<0.0001	<0.0001	<0.0001	<0.0001	<0.0001	<0.0001
Lack of Fit	0.79	0.85	0.4	0.6853	0.1615	0.7058
R^2	0.9905	0.9875	0.9846	0.9898	0.992	0.9795
Adjusted R^2	0.9783	0.9713	0.9648	0.9768	0.9818	0.9888
Predicted R^2	0.9571	0.8042	0.8569	0.9424	0.956	0.9771
Adeq. Prec.	26.33	22	18.6	30.14	26.77	24.56

According to the results shown in Table 4, factor A (RHA) has a substantial impact on the responses TS, UTS, HD, and CS ($p < 0.05$), while it has only a marginal impact on FS ($p > 0.05$). The *p*-value for component B (GP) is less than 0.05, while the *p*-value for factor C (temperature) is also less than 0.05. The contributions of RHA and temperature to all of the responses are important, as the conclusion suggests. As the *p*-values for the cross interactions between the factors (AB, AC, and BC) are all greater than 0.05 for each of the attributes, it can be deduced that the contributions of the cross interactions to the responses are not significant. With the exception of microhardness, the square interaction A^2 had a substantial influence on all of the responses of the attributes. B^2 had a substantial effect on all of the responses, with the exception of the microhardness and compressive strength measurements. It has been shown that the influence of interaction C^2 is significant for each and every response (*p*-value less than 0.05).

3.2.2. Mathematical Models

The mathematical models for yield strength, ultimate tensile strength, microhardness, flexural strength, impact strength, and compressive strength are represented by Equations (1)–(6), respectively. The models show that the coefficients of components A and C both have a positive value. This indicates that factors A (RHA) and C (temperature) have a consequentially constructive impact (one that is synergistic with the responses). The only instance in which component B has a negative coefficient is in the context of microhardness; this indicates that factor B acts in a manner that is hostile to microhardness. The ensuing effects of square interaction A^2 exhibited a negative impact on YS, UTS, FS, and CS, but a good contribution to HD. It can be deduced from the models that the contributions of B^2 and C^2 are in opposition to all of the responses. When it comes to the cross interactions, AB is antagonistic to YS, UTS, and HD, while it has a synergistic relationship with FS, IS, and CS. When it comes to interaction AC, the contribution is antagonistic toward UTS, HD, FS, and IS, but synergistic in terms of YS and CS. Due to this, factor BC had a consequent posi-

tive effect on the variables YS, UTS, and HD, while it had a resultant negative contribution to the variables FS, IS, and CS.

$$YS = -4100.3063 + 98.4722\ A + 85.3604\ B + 12.3758\ C - 1.3889\ AB + 0.0017\ AC + 0.0063\ BC - 6.9963\ A^2 \\ - 7.3391\ B^2 - 0.0092\ C^2 \tag{1}$$

$$UTS = -6114.3833 + 158.7500\ A + 88.1271\ B + 17.5603\ C - 1.4028\ AB - 0.0483\ AC + 0.0100\ BC - 8.4741\ A^2 \\ - 7.7719\ B^2 - 0.0126\ C^2 \tag{2}$$

$$HD = -703.3326 + 3.7037\ A - 1.4333\ B + 2.2863\ C - 0.0972\ AB - 0.0011\ AC + 0.0150\ BC + 0.0086\ A^2 \\ - 0.2078\ B^2 - 0.0016\ C^2 \tag{3}$$

$$FS = -3856.2750 + 58.0833\ A + 56.9646\ B + 11.9008\ C + 1.3889\ AB - 0.0017\ AC - 0.0006\ BC - 4.2000\ A^2 \\ - 6.2844\ B^2 - 0.0087\ C^2 \tag{4}$$

$$IS = -33.5943 + 0.5969\ A + 1.0940\ B + 0.1127\ C + 0.0001\ AB + 0.0007\ AC - 0.0000\ BC - 0.0814\ A^2 \\ - 0.1002\ B^2 - 0.0001\ C^2 \tag{5}$$

$$CS = -7131.0729 + 94.2222\ A + 31.7292\ B + 21.0042\ C + 0.0278\ AB + 0.0078\ AC - 0.0069\ BC - 6.2778\ A^2 \\ - 0.2109\ B^2 - 0.0153\ C^2 \tag{6}$$

3.3. Response Surface Analysis and Contour Plots

3.3.1. Assessment of Effect of the Interaction between Rice Husk Ash and Glass Powder (at 700 °C Constant Temperature) on Responses

The effect of the interaction between rice husk ash and glass powder on the yield tensile strength, ultimate tensile strength, flexural strength, microhardness, impact strength, and compressive strength is showcased in Figure 1a–f, respectively. As observed in Figure 1a–d, the blend of 3–7.5% RHA and 2–6% GP sparked improvement in the responses. The strength increase observed from 3–7.5% RHA and 2–6.0% GP is similar to the findings of Ahamed et al. [34], in which progressive enhancement of strength was noticed with 3–9 percent RHA. Likewise, Adediran et al. [35] reported an increment in tensile strength when glass particulate was introduced into Al-6061 melt in a similar manner, with these findings between 2 and 6 percent GP in this study. Adediran et al. [35]; Ahamed et al. [34] linked the increased strength to the coexistence of the two types of particulates as well as good adhesion with the matrix via particle strengthening mechanisms. Moderate viscosity resulting from moderate casting temperature was linked to the improved tensile strength of the composite when temperature was between 600 and 700 °C [36].

On the other hand, the combination of 7.5–12% RHA and 6–10% GP (Figure 1a–f) led to strength reduction. The reduction in strength is associated with the high density of the particles and the resulting clustering of particles within the matrix, as reported by Roether and Boccaccini [37]. Virkunwar et al. [38] associated the findings to poor wettability existing between particulates, and they observed a decrease in tensile strength when RHA exceeded 8 percent in their study. In Figure 1d, a progressive improvement in hardness is shown when 3–12% RHA is combined with 2–10% GP in the matrix at a constant temperature of 700 °C. Mishra et al. [39] revealed the significance of RHA in the improvement of the hardness of aluminum alloy composites. Verma and Vettivel [40] carried out response surface optimization of Al-7075 reinforced with RHA and B_4C. Interaction between 1–5% RHA and 1–5% B_4C engendered progressive improvement in microhardness. The surface plot of the interaction between RHA and B_4C in the study is in sync with the result of the surface plot depicted for the interaction between GP and RHA in the present study. The accretion recorded is connected to an increment in particulate presence and the improved cohesion between particles. Saravanan and Senthilkumar [41] validated the use of GP in this study, as similar accretion in hardness with progressive assimilation of GP was reported.
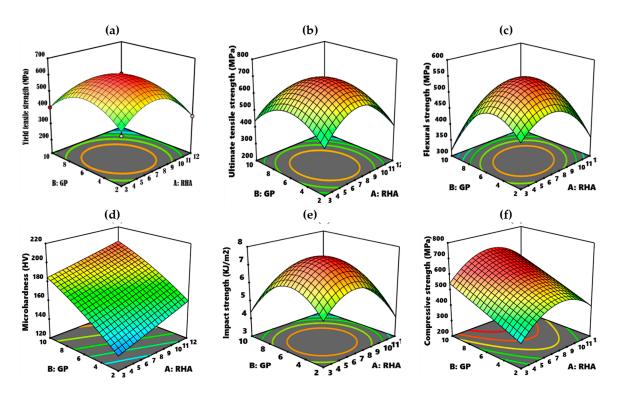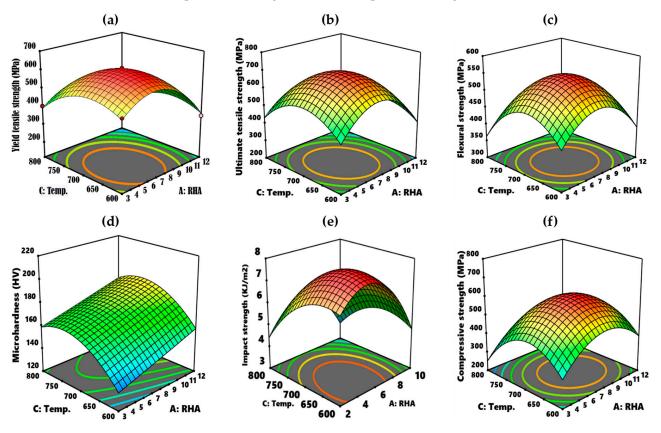
Figure 1. Response surface revealing effects of interaction of rice husk ash vs. glass powder at 700 °C constant temperature on (**a**) yield strength, (**b**) ultimate tensile strength, (**c**) flexural strength, (**d**) microhardness, (**e**) impact strength, (**f**) compressive strength.

The 3–12% RHA blended with 2–6% GP is responsible for the improvement in compressive strength as indicated in Figure 1f. The improvement in compressive strength is attributable to compaction and reduced interparticle distance based on the even dispersion of the particles within the matrix, resulting in increased dislocation density and consequently improved strength. In addition, such an improvement in strength is attainable on account of reduced interparticle distance within the composite structure, consequently improving compaction. Senapati et al. [42] reported a progressive rise in the compressive strength of aluminum composites prepared with 2–12 wt.% RHA. The blend of fly ash and RHA, as reported by Saravanan and Kumar [43], has considerable input in improving the compressive strength of the Al-Si LM6 alloy. The authors Ali and Motgi [44] demonstrated the potential of RHA in improving the compressive strength of the AlSi 10 Mg matrix by assimilation of 2–12% RHA in the matrix. However, the same dosage of RHA combined with 6–10% GP triggers strength reduction. The deterioration occurred due to the brittle nature of the particulate. Akinwande et al. [23] claimed that at higher particle densities for glass powder, there is a tendency for the brittle nature of the particulate to take dominance, leading to a reduction in density.

3.3.2. Assessment of Effect of the Interaction between Rice Husk Ash and Temperature on Responses When Maintaining GP at 6% Constant Dosage

The influence of the interaction between rice husk ash and stirring temperature (maintaining GP at 6%) on the yield tensile strength, ultimate tensile strength, flexural strength, microhardness, impact strength, and compressive strength is illustrated in Figure 2a–f, respectively. The response plots portrayed in Figure 2a–f show that the responses were improved with the introduction of 3–7.5% RHA at 600–700 °C. This study revealed that 600–700 °C favors improvement of impact strength whereas 700–800 °C is detrimental to the strength. The influence of temperature on the strength performance of aluminum composites elucidated in Mathur and Barnawal [45] showed that an increase in temperature between 700 and 725 °C was beneficial to the strength property evaluated, while between 725 and 750 °C, the strength value declined. The observation substantiates the findings of
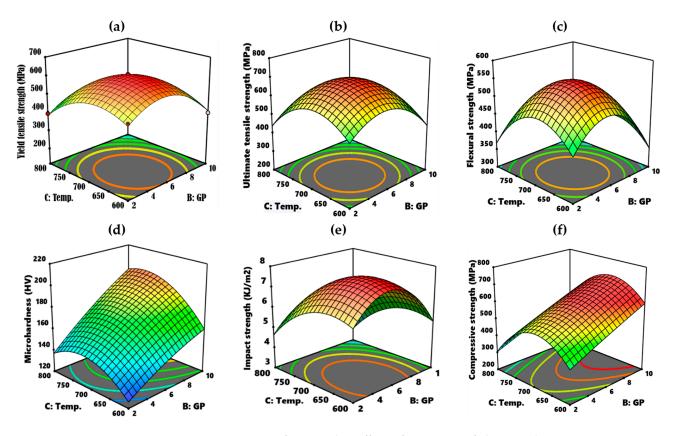
this study as regards how temperature affects strength. The decline in strength is associated with particulate coagulation and the possible storage of residual stress.

Figure 2. Response surface revealing effects of interaction of rice husk ash vs. stirring temperature at 6% constant GP dosage on (**a**) yield strength, (**b**) ultimate tensile strength, (**c**) flexural strength, (**d**) microhardness, (**e**) impact strength, (**f**) compressive strength.

3.3.3. Assessment of Effect of the Interaction between Glass Powder and Temperature on Responses When Maintaining RHA at 7.5% Fixed Proportion

Figure 3a–f, respectively, present the surface plots for responses of yielding tensile strength, ultimate tensile strength, flexural strength, microhardness, impact strength, and compressive strength as functions of the input variables, glass powder and stirring temperature, when holding RHA at 7.5%. It is observed in Figure 3a–e that a dosage of 2–6% GP at stirring temperature of 600–700 °C ensured enhancement of the strength response. The viscosity of a metal melt is dependent on casting temperature, and it influences the properties of the developed composite [46]. At lower viscosity, the reinforcing particles have lower mobility within the melt, causing segregation, agglomeration, and clustering. If the viscosity is high due to a high temperature, particles possess a high amount of kinetic energy with the possibility of even dispersion. At much higher temperatures, there is a tendency for gas entrapment. However, determining the moderate casting temperature for even casting is not an easy task. In this study, temperatures between 600 and 700 °C seem moderate, beyond which there is strength reduction.

In Figure 3d,f for microhardness and compressive strength, 2–10% GP engendered improvement of hardness at 600–700 °C stirring temperature, while the same proportion of GP at 700–800 °C is detrimental. According to Mathur and Barnawal [45], temperatures between 700 and 725 °C were favorable to hardness and compressive strength, while temperatures between 725 and 750 °C caused a decrease in the response values due to the likely presence of defects such as microcracks, surface microporosity, and weakened bonds in the matrix. In this study, the temperature range of 600 and 700 °C favors enhancement

of hardness and compressive strength, while the temperature range of 700–800 °C is detrimental to the properties.

Figure 3. Response surface revealing effects of interaction of glass powder vs. stirring temperature at 7.5% RHA constant loading on (**a**) yield strength, (**b**) ultimate tensile strength, (**c**) flexural strength, (**d**) microhardness, (**e**) impact strength, (**f**) compressive strength.

3.4. Optimization and Validation

The response surface approach is a useful statistical and mathematical tool for optimizing multi-response parameters that have been specified by constraints, according to Awolusi et al. [46], and it has found application in a number of experimental and optimization analyses [47–52]. In the current investigation, Design-Expert software version 13 was applied for the purpose of conducting a multi-response optimization approach using the predetermined criteria shown in Table 5.

Table 5. Optimization criteria.

Name	Goal	Lower Limit	Upper Limit	Lower Weight	Upper Weight
A: RHA	is in range	3 wt.%	12 wt.%	1	1
B: GP	is in range	2 wt.%	10 wt.%	1	1
C: temperature	is in range	600 °C	800 °C	1	1

While the primary objective was to obtain the highest possible values for the strength parameters, the input variables A, B, and C were constrained to the ranges shown in Table 5.

The optimum experimental conditions for the multi-response optimization as predicted by the software are 7.24185~7.2 wt.% RHA, 6.21163~6.2 wt.% GP, and 695.126~695 °C for temperature (Figure 4). The predicted response values are presented in Table 6.
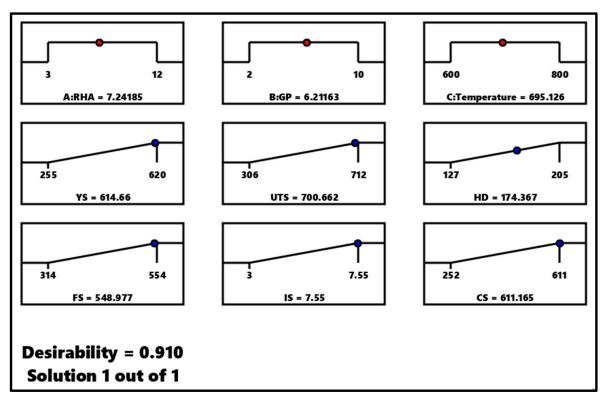
Figure 4. Optimization ramp indicating optimum combination and predicted responses at desirability of 0.910.

Table 6. Validation table.

Properties	Predicted Values	Confirmation Values	% Error
Yield tensile strength (MPa)	614.66	603.4	−1.87
Ultimate tensile strength (MPa)	700.662	697.3	−1.91
Flexural strength (MPa)	548.977	556.1	+1.30
Microhardness (Hv)	174.367	183	+4.95
Impact strength (KJ/m^2)	7.55	7.7	+2.12
Compressive strength	611.165	598.3	−2.10

In the validation of the model, a confirmation experiment was carried out at optimum conditions of 7.2% RHA, 6.2% GP, 695 °C and triplicate samples were tested for each property. The experimental value obtained for each response is highlighted in Table 6. The estimated errors for each of the five responses are less than 5%, confirming the models to be statistically fit for the prediction of responses.

4. Conclusions

In this study, response surface analysis was engaged in the design of experiment, analysis of properties, modeling, and optimization of the mechanical performance of Al-7075 hybridized with green fillers (RHA and GP). According to our findings:

1. The results of the analysis of variance (ANOVA) showed that the three parameters, RHA proportion, GP dosage, and stirring temperature, had significant effects on yield, ultimate tensile, flexural, compressive and impact strengths, as well as microhardness. The probability value for each response was less than 0.05, indicating that the parameters' effects were significant.
2. It was determined that the model that had been built for each response parameter was statistically significant and appropriate for use in the prediction of the responses.

3. The surface plots which present the relation between the response variables and the input variables revealed that the trend of the properties is dependent on the input variables.

4. The optimal experimental conditions for the multi-response optimization are a temperature of 598.06 °C, 8.47 weight percent of GP, and 0.28 weight percent of RHA. The values that are projected are as follows: yield tensile strength of 614.66 MPa, ultimate tensile strength of 700.662 MPa, flexural strength of 548.977 MPa, microhardness of 174.367 Hv, impact strength of 7.55 KJ/m^2, and compressive strength of 7.55 KJ/m^2. The model was shown to be accurate when it was validated by an experiment that produced the results 603.4 MPa, 697.3 MPa, 556.1 MPa, 183 Hv, and 7.7 KJ/m^2, and 598.3 MPa, correspondingly.

In that case, the developed models were affirmed to be adequate for response predictions, and equally, the optimum condition that yielded the highest desirability is fit for desired composite development.

Author Contributions: O.S.A. and A.A.A. (Abayomi Adewale Akinwande): Conceptualization, data curation, methodology, formal analysis, article writing and literature review, manuscript draft, editing. O.A.B., A.A.A. (Adeolu Adesoji Adediran) and O.O.S.: data curation, article writing and literature review, manuscript draft, editing. V.R.: methodology, formal analysis, article writing and literature review, manuscript draft, editing. All authors have read and agreed to the published version of the manuscript.

Conflicts of Interest: The authors declare no conflict of interest that may influence representation or interpretation of reported research results.

References

1. Selvam, P.; Sasikumar, R.; Natarajan, E. Superior material properties of hybrid filler reinforced aluminium MMC through double layer feeding technique adopted in bottom tapping stir casting. *High Temp. Mater. Process.* **2018**, *22*, 249–258. [CrossRef]
2. Fanani, E.W.A.; Surojo, E.; Prabowo, A.R.; Akbar, H.I. Recent progress in hybrid aluminium composite manufacturing and application. *Metals* **2021**, *11*, 1919. [CrossRef]
3. Ahmad, A.; Lajis, M.A.; Yusuf, N.K.; Rahim, S.N.A. Statistical optimization by the response surface methodology of direct recycled aluminium-alumina metal matrix composite (MMC-AL$_R$) employing the metal forming process. *Processes* **2020**, *8*, 805. [CrossRef]
4. Sharma, A.K.; Bhandari, R.; Aherwar, A.; Rimasauskiene, R.; Bretotean, C.P. A study of advancement in application opportunity of aluminium metal matrix composites. *Mater. Today Proc.* **2020**, *26*, 2419–2424. [CrossRef]
5. Johnu, J.S.; Venkatesan, K.; Kuppan, P.; Ramanujam, R. Hybrid aluminium metal matrix composite reinforced with SiC and TiB$_2$. *Procedia Eng.* **2014**, *97*, 1018–1026. [CrossRef]
6. Sharma, R.; Sharma, P.; Singh, G. Dry sliding behavior of aluminium alloy reinforced with hybrid ceramic particles. *Int. J. Multidiscip. Res. Dev.* **2015**, *2*, 485–491.
7. Radha, A.; Vijayakumar, K.R. An investigation of mechanical and wear properties of AA 6061 reinforced with silicon carbide and graphene nano particles-particulate reinforced composites. *Mater. Today Proc.* **2016**, *3*, 2247–2253. [CrossRef]
8. Pitchayyapillai, G.; Seenikannan, P.; Raja, K.; Chandrasekaran, K. Al6061 hybrid metal matrix composite reinforced with alumina and molybdenum sulphide. *Adv. Mater. Sci. Eng.* **2016**, *2016*, 6127624. [CrossRef]
9. Raj, P.; Deepanraj, B.; Senthilkumar, N.; Tamizharasan, T. A study on effect of primary and secondary reinforcement in hybrid metal composite. *AIP Conf. Proc.* **2022**, *2393*, 020222. [CrossRef]
10. Bucham, J.O.; Igbax, S.I.; Aliyu, A.B. Hybrid aluminium alloy (Aa6061) composite mechanical properties investigation. *United Int. J. Res. Technol.* **2022**, *3*, 44–48.
11. Vijayakumar, K.; Prabhu, L.; Subin, B.S.; Satheen, S.; Vaishnav, K. Development of hybrid aluminium metal matrix composites for marine applications. *IOP Conf. Ser. Mater. Sci. Eng.* **2020**, *993*, 012016. [CrossRef]
12. Dwivedi, S.P.; Srivastava, A.K.; Maurya, A.K.; Sahu, R. Microstructure and mechanical behavior of Al/SiC/Agro-waste RHA hybrid metal matrix composite. *J. Compos. Adv. Mater.* **2020**, *30*, 43–47.
13. Singh, P.; Mishra, R.K.; Singh, B. Mechanical characterization of eggshell ash and boron carbide reinforced ZA-27 hybrid metal matrix composites. *Process Mech. Eng. C* **2021**, *236*, 1766–1779. [CrossRef]

14. Mugutkar, H.; Tamiloli, N.; Kohir, V.V. Comparative analysis of mechanical studies of Al7075 hybrid metal composites as a functionality of SiO$_2$ in RHA. *Acad. J. Manuf. Eng.* **2022**, *20*, 19–23.

15. Subramaniam, B.; Natarajan, B.; Kaliyaperumal, B.; Jerold, S.; Chelladurai, S. Investigation on mechanical properties of aluminium 7075-boron carbide-coconut shell fly ash reinforced hybrid metal matrix composites. *China Foundry* **2018**, *15*, 449–457. [CrossRef]

16. Dwivedi, S.S.; Dwivedi, G. Utilization of RHA in development of green composite material using RSM. *J. Mech. Behav. Mater.* **2019**, *28*, 20–28. [CrossRef]

17. Lei, Z. Research on mechanical properties of the waste glass/waste aluminium wearable materials. *Adv. Mater. Res.* **2012**, *460*, 424–427. [CrossRef]

18. Hendronursito, Y.; Ojahan, T.; Anshori, A.; Yunanto, A. Optimization of stir casting of aluminium matrix composites (AMCs) with filler of recycled glass powder (RGP) for the mechanical properties. *J. Mech. Eng. Sci. Technol.* **2020**, *4*, 101–114. [CrossRef]

19. Balogun, O.A.; Akinwande, A.A.; Adediran, A.A.; Ogunsanya, O.A.; Ademati, A.O.; Kumar, M.S.; Erinle, T.J.; Akinlabi, E.T. Microstructure and particle size effects on selected mechanical properties of waste glass-reinforced aluminium matrix composites. *Mater. Today Proc.* **2022**, *62*, 4589–4598. [CrossRef]

20. Shivalingaiah, K.; Nagarajaiah, V.; Selvan, C.P.; Kariappa, S.T.; Chandrashekarappa, N.G.; Lakshmikanthan, A.; Chandrashekarappa, M.P.G. Stir casting process analysis and optimization for better properties in Al-MWCNT-GR-based hybrid composites. *Metals* **2022**, *12*, 1297. [CrossRef]

21. Sahu, M.K.; Sahu, R.K. Experimental investigation, modeling, and optimization of wear parameters of B4C and fly-ash reinforced aluminium hybrid composite. *Front. Phys.* **2020**, *8*, 219. [CrossRef]

22. Akinwande, A.A.; Balogun, O.A.; Adediran, A.A.; Adesina, O.S.; Romanovski, V.; Jen, T.C. Experimental analysis, statistical modeling, and parametric optimization of quinary-(CoCrFeMnNi)$_{100-x}$/TiC$_x$ high-entropy-allo (HEA) manufactured by laser additive manufacturing. *Results Eng.* **2022**, *17*, 100802. [CrossRef]

23. Akinwande, A.A.; Balogun, O.A.; Romanovski, V. Modelling, multi-response optimization, and performance reliability of green metal composites produced from municipal wastes. *Environ. Sci. Pollut. Res.* **2022**, *29*, 61027–61048. [CrossRef]

24. Adediran, A.A.; Akinwande, A.A.; Balogun, O.A.; Olorunfemi, B.J.; Kumar, M.S. Optimization studies of stir casting parameters and mechanical properties of TiO$_2$ reinforced AL 7075 composite using response surface methodology. *Sci. Rep.* **2021**, *11*, 19860. [CrossRef] [PubMed]

25. Balogun, O.A.; Akinwande, A.A.; Ogunsanya, O.A.; Ademati, A.O.; Adediran, A.A.; Erinle, T.J.; Akinlabi, E.T. Central composite design and optimization of selected stir casting parameters on flexural strength and fracture toughness of mTiO$_2$p/Al 7075 composites. *Mater. Today Proc.* **2022**, *62*, 4574–4583. [CrossRef]

26. Kumar, K.S.; Baskar, K. Response surfaces for fresh and hardened properties of concrete with E-wastes (HIPS). *J. Waste Manag.* **2014**, *2014*, 517219. [CrossRef]

27. Nwose, S.A.; Edoziuno, F.O.; Osuji, S.O. Statistical analysis and response surface modelling of the compressive strength inhibition of crude oil in concrete test cubes. *Alger. J. Eng. Technol.* **2021**, *4*, 99–107. [CrossRef]

28. Peasura, P. Application of response surface methodology for modelling of postweld heat treatment process in a pressure vessel steel ASTM A516 grade 70. *Sci. World J.* **2015**, *2015*, 318475. [CrossRef] [PubMed]

29. *ASTM E 8/E8M-21*; Standard Test Methods for Tension Testing of Metallic Materials. ASTM International: West Conshohocken, PA, USA, 2021. [CrossRef]

30. *ASTM A 370-20*; Standard Test Methods and Definitions for Mechanical Testing of Steel Products. ASTM International: West Conshohocken, PA, USA, 2020. [CrossRef]

31. *ASTM E 384-17*; Standard Test Methods for Micro-Identation Hardness of Materials. ASTM International: West Conshohocken, PA, USA, 2017. [CrossRef]

32. *ASTM E 3-11*; Standard Guide for Preparation of Metallographic Specimens. ASTM International: West Conshohocken, PA, USA, 2017. [CrossRef]

33. *ASTM E 9-09*; Standard Test Method of Compression Testing of Metallic Materials at Room Temperature. ASTM International: West Conshohocken, PA, USA, 2018. [CrossRef]

34. Ahamed, A.A.; Ahmed, R.; Hossain, M.B.; Billah, M. Fabrication and characterization of aluminium-rice husk ash composites prepared by stir casting method. *Rajshahi Univ. J. Sci. Eng.* **2016**, *44*, 9–18. [CrossRef]

35. Adediran, A.A.; Akinwande, A.A.; Balogun, O.A.; Adesina, O.S.; Olayanju, A.; Mojisola, T. Evaluation of the properties of Al-6061 alloy reinforced with particulate waste glass. *Sci. Afr.* **2021**, *12*, e00812. [CrossRef]

36. Shin, S.; Park, H.; Park, B.; Lee, S.B.; Lee, S.K.; Kim, Y.; Cho, S.; Jo, I. Dispersion mechanism and mechanical properties of SiC reinforcement in aluminium matrix composite through stir and die casting processes. *Appl. Sci.* **2021**, *11*, 952. [CrossRef]

37. Roether, J.A.; Boccaccini, A.R. Dispersion-reinforced glass and glass-ceramic matrix composites. In *Handbook of Ceramic Composites*; Bansal, N.P., Ed.; Springer: Boston, MA, USA, 2005. [CrossRef]

38. Virkunwar, A.K.; Ghosh, S.; Basak, R.; Rao, A.S. Study of mechanical and tribological characteristics of aluminium alloy reinforced with rice husk ash. In Proceedings of the TRIBOINDIA-2018, An International Conference on Tribology, Mumbai, India, 13–15 December 2018. [CrossRef]

39. Mishra, P.; Mishra, P.; Rana, R.S. Effect of rice husk ash reinforcement on mechanical properties of aluminium alloy (LM 6) matrix composites. *Mater. Today Proc.* **2017**, *5*, 6018–6022. [CrossRef]

40. Verma, N.; Vettivel, S.C. Characterization and experimental analysis of boron carbide and rice husk ash reinforced AA7075 aluminium alloy hybrid composite. *J. Alloys Compd.* **2018**, *741*, 981–998. [CrossRef]

41. Saravanan, S.D.; Senthilkumar, M. Mechanical behavior of aluminium (AlSi10Mg)-RHA composite. *Int. J. Eng. Technol.* **2014**, *5*, 4834–4840.

42. Senapati, A.K.; Sahoo, S.K.; Singh, S.; Sah, S.; Padhi, P.R.; Satapathy, N. A comparative investigation on physical and mechanical properties of MMC reinforced with waste materials. *Intern. J. Eng. Adv. Technol.* **2017**, *6*, 161–169.

43. Saravanan, S.D.; Kumar, M.S. Effect of mechanical properties on rice husk ash reinforced aluminium alloy (AlSi10Mg) matrix composites. *Procedia Eng.* **2013**, *64*, 1505–1513. [CrossRef]

44. Ali, S.A.; Motgi, B.S. A study on mechanical properties of Al 6068 based metal matrix composite reinforced with rice husk ash (RHA) and silicon carbide (SiC). *Int. J. Mod. Trends Sci. Technol.* **2021**, *7*, 71–78. [CrossRef]

45. Mathur, S.; Barnawal, A. Effect of process parameter of stir casting on metal matrix composites. *Int. J. Sci. Res.* **2013**, *2*, 395–398.

46. Awolusi, T.F.; Oke, L.O.; Akinkurolere, O.O.; Uban, D.P.; Bamisaye, R.T.; Aluko, O.G. The application of response surface methodology in understanding the compressive strength and water absorption capacity of sandcrete. *Silicon* **2020**, *13*, 4123–4132. [CrossRef]

47. Penjumras, P.; Rahman, R.A.; Talib, R.A.; Abdan, K. Response surface methodology for the optimization of preparation of biocomposites based on poly(lactic acid) and durian peel cellulose. *Sci. World J.* **2015**, *2015*, 293609. [CrossRef]

48. Akinwande, A.A.; Folorunso, D.O.; Balogun, O.A.; Romanovski, V. Mathematical modelling, multi-objective optimization, and compliance reliability of paper-derived eco-composites. *Environ. Sci. Pollut. Res.* **2022**, *29*, 70135–70157. [CrossRef]

49. Akinwande, A.A.; Folorunso, D.O.; Balogun, O.A.; Danso, H.; Romanovski, V. Paperbricks produced from wastes: Modeling and optimization of compressive strength by response surface approach. *Environ. Sci. Pollut. Res.* **2022**, *30*, 8080–8097. [CrossRef] [PubMed]

50. Akinwande, A.A.; Adediran, A.A.; Balogun, O.A.; Yibowei, M.E.; Barnabas, A.A.; Talabi, H.K.; Olorunfemi, B.J. Optimization of selected casting parameters on the mechanical behavior of Al 6061/glass powder composites. *Heliyon* **2022**, *8*, e09350. [CrossRef] [PubMed]

51. Adesina, O.S.; Adediran, A.A.; Akinwande, A.A.; Daramola, O.O.; Sanyaolu, O. Modelling and optimizing tensile behavior of developed aluminium hybrid composite. *Surf. Rev. Lett.* **2022**, *29*, 2250120. [CrossRef]

52. Ogunbiyi, O.; Tian, Y.; Akinwande, A.A.; Rominiyi, A.L. AA7075/HEA composites fabricated by microwave sintering: Assessment of the microstructural features and response surface optimization. *Intermetallics* **2023**, *155*, 107830. [CrossRef]